

Article

# On the Constant-Roll Tachyon Inflation with Large and Small $\eta_H$

Qin Fei, Waqas Ahmed \* and Zhen-Lai Wang

School of Mathematics and Physics, Hubei Polytechnic University, Huangshi 435003, China

\* Correspondence: waqasmit@hbpu.edu.cn

**Abstract:** We study the constant-roll tachyon inflation with large and small  $\eta$ . In previous studies, only the constant-roll tachyon inflation with small  $\eta$  is consistent with the observations. We find that the duality between the constant-roll tachyon inflation with large and small  $\eta$  may exist. The apparent duality suggests that the constant-roll tachyon inflationary model with large  $\eta$  may also be consistent with the observations. By fitting the spectral tilde  $n_s$  and tensor to scalar ratio  $r$ , which is a measure of primordial gravitational waves with the observations, we get small and large  $\eta$  in this range  $-0.01629 \leq \eta_H \leq -0.00079$  and  $3.00081 \leq \eta_H \leq 3.01621$  at the  $2\sigma$  C.L for  $N = 60$  e-folds.

**Keywords:** ultra-slow-roll inflation; cosmological constraints; duality

## 1. Introduction

The WMAP [1], and Planck [2] observations indicate that the inflation era in the early universe is one of the most critical parts of standard cosmology. Inflation not only solves the horizon, flatness, and monopole problems but also plays an essential role in the generation of super-horizon fluctuations, which are considered to be the origin of the large-scale structures which leave imprints of the CMB [3–7]. Due to the uncertainties in reheating physics, the amount of inflation must be large enough to solve the problems mentioned above, which requires nearly flat potential. The temperature and polarization measurements on the CMB anisotropy suggest spectral tilde  $n_s = 0.9642 \pm 0.0042$  and tensor to scalar ratio  $r \leq 0.08$  in  $2\text{-}\sigma$  C.L [2,8].

The constant-roll inflation recently attracted much attention because cosmological equations can be solved more easily. The model differs from the typical slow-roll inflationary models, where the second slow-roll parameter  $\eta$  is tiny instead of constant [9,10]. In particular, when the inflationary potential becomes very flat, the inflation almost stops rolling, we get  $\eta \approx 3$ , and we call this model ultra-slow roll [11,12]. Constant roll solutions generalize “ultra-slow-roll” dynamics, where the first slow roll parameter is small, but the second slow roll parameter  $\eta$  is larger than unity. During inflation  $\eta > 1$ , the slow roll parameter  $\epsilon_H$  decreases with time; so, to calculate the power spectra, one can still use the standard method of Bessel function approximation. If one can neglect the contribution of  $\epsilon_H$ , there is a duality between the constant-roll inflation and the slow-roll inflation [13,14]. On the other hand, the observational data favor  $\eta_H$ , which is small [15–17], and which contradicts the duality relation.

The constant-roll inflationary models in the canonical scalar field are in line with Planck’s 2018 data; if we do not persist, the only available scalar field is the Higgs field. However, in Higgs field theory, the monomial potentials with quartic power are ruled out, but quadratic and linear still have some parametric space; for details, see Refs [18,19]. In quartic potential, tensor-to-scalar ratio  $r = 0.19$ , so the model is excluded in the  $2\sigma$  C.L. In order to make an  $r$  prediction consistent with Planck 2018 data a non-canonical scalar field is used to drive the inflation [16,20–26].

Apart from a canonical scalar field to drive inflation, another interesting inflationary model is tachyonic inflation. In string theory, the effective scalar field with a nonlinear



**Citation:** Fei, Q.; Ahmed, W.; Wang, Z.-L. On the Constant-Roll Tachyon Inflation with Large and Small  $\eta_H$ . *Symmetry* **2022**, *14*, 2670. <https://doi.org/10.3390/sym14122670>

Academic Editors: Roberto Passante and Vasilis Oikonomou

Received: 10 October 2022

Accepted: 8 December 2022

Published: 16 December 2022

**Publisher’s Note:** MDPI stays neutral with regard to jurisdictional claims in published maps and institutional affiliations.



**Copyright:** © 2022 by the authors. Licensee MDPI, Basel, Switzerland. This article is an open access article distributed under the terms and conditions of the Creative Commons Attribution (CC BY) license (<https://creativecommons.org/licenses/by/4.0/>).

kinetic term, which describes the tachyon condensate, also drives inflation and provides the almost scale invariant power spectrum [27–29]. The current observation still does not address the scalar field’s nature, so considering tachyon inflation and its physical implications is an exciting study. Tachyon inflation in the context of the slow-roll condition can be seen in ref [25,30]. When the slow-roll approximation is violated in constant-roll inflation, the scalar and tensor perturbations equations derived in the slow-roll approximation case also require modification. Comparing with other non-minimal inflation models, such as the scalar-tensor theory and derivative coupling inflation model, tachyonic inflation has only one freedom: the constant-roll condition can fully determine the inflationary potential, and more information of the tachyonic inflation will be obtained.

In this paper, we will study the constant-roll tachyon inflation with the second slow-roll parameter  $\eta$  being a constant. Then, we study the duality between large and small  $\eta$  for the constant-roll tachyon inflation, and compare the result with the Planck 2018. The spectral tilde  $n_s$  and tensor to scalar ratio  $r$  consistent with Planck required  $-0.01629 \leq \eta_H \leq -0.00079$  and  $3.00081 \leq \eta_H \leq 3.01621$  at the  $2\sigma$  C.L, for  $N = 60$  e-folds.

The paper is organized as follows. In Section 2, we review the constant roll of Higgs inflation and discuss the duality property. In Section 3 we review the tachyon inflation. Sub Section 3 contains scalar perturbation, tensor perturbation, and the discussion of duality between the slow-roll inflation and large constant  $\eta$ . Here we also provide the example of tachyon inflation in the constant-roll background and fit the observational constraints. The conclusions are drawn in Section 4.

### 2. Duality in Canonical Inflation

In this section, we review the constant-roll inflation with the canonical field, and show the duality between the small and large  $\eta$ . For the canonical scalar field, the action is

$$S = \int d^4x \sqrt{-g} \left[ \frac{M_{\text{pl}}^2}{2} R - \frac{1}{2} g^{\mu\nu} \partial_\mu \phi \partial_\nu \phi - V(\phi) \right], \tag{1}$$

where  $R$  is Ricci scalar,  $V(\phi)$  is the potential which is a function canonical scalar field  $\phi$  and  $M_{\text{pl}} = \sqrt{8\pi G}$  is the reduced Planck mass. In this paper, we choose  $M_{\text{pl}} = c = 1$ . With the Friedmann-Robertson-Walker metric, the background equations are

$$3H^2 = \frac{\dot{\phi}^2}{2} + V(\phi), \tag{2}$$

$$\frac{dH}{d\phi} = -\frac{\dot{\phi}}{2}, \tag{3}$$

$$\ddot{\phi} + 3H\dot{\phi} + \frac{\partial V}{\partial \phi} = 0. \tag{4}$$

For the slow-roll parameters, we use the Hubble flow slow-roll parameters [31]

$${}^n\beta_H = 2 \left( \frac{(H_{,\phi})^{n-1} H_{,\phi}^{(n+1)}}{H^n} \right)^{1/n}, \tag{5}$$

where  $H_{,\phi}^{(n)} = d^n H / d\phi^n$ . In particular, the first two slow-roll parameters are

$$\epsilon_H = 2 \left( \frac{H_{,\phi}}{H} \right)^2, \quad \eta_H = \frac{2H_{,\phi}^{(2)}}{H}. \tag{6}$$

The constant-roll inflation takes one of the slow-roll parameters as a constant. Usually, the slow-roll parameter  $\eta_H$  is chosen as a constant [10,32],

$$\eta_H = \text{Constant}. \quad (7)$$

With the help of the background Equations (2)–(4), the slow-roll parameters can be expressed as

$$\epsilon_H = 2 \left( \frac{H_{,\phi}}{H} \right)^2 = -\frac{\dot{H}}{H^2}, \quad (8)$$

$$\eta_H = \frac{2H_{,\phi}^{(2)}}{H} = -\frac{\ddot{\phi}}{H\dot{\phi}} = -\frac{\ddot{H}}{2H\dot{H}}. \quad (9)$$

The scalar perturbations are governed by the Mukhanov-Sasaki equation [33,34],

$$v_k'' + \left( k^2 - \frac{z''}{z} \right) v_k = 0, \quad (10)$$

where  $\tau = \int dt/a$  is the conformal time,  $z = a\dot{\phi}/H$ , and  $v_k = z\zeta_k$ ,  $\zeta_k$  is the scalar perturbation in the Fourier space and a “prime” means the derivative with respect to the conformal time  $\tau$ . To the first order of  $\epsilon_H$  and keeping  $\eta_H$  as a constant, Equation (10) can be expressed as

$$v_k'' + \left( k^2 - \frac{v^2 - 1/4}{\tau^2} \right) v_k = 0, \quad (11)$$

where [32]

$$v \approx \frac{1}{2} |2\eta_H - 3| + \frac{(2\eta_H^2 - 9\eta_H + 6)\epsilon_H}{|2\eta_H - 3|}. \quad (12)$$

Regarding  $v$  as a constant, Equation (11) can be transferred to the Bessel equation. By this method, the power spectrum of the scalar perturbation is

$$P_\zeta = \frac{k^3}{2\pi^2} |\zeta_k|^2 = \frac{2^{2\nu-3}}{2\epsilon_H} \left[ \frac{\Gamma(\nu)}{\Gamma(3/2)} \right]^2 (1 + \epsilon_H)^{1-2\nu} \left( \frac{H}{2\pi} \right)^2 \left( \frac{k}{aH} \right)^{3-2\nu}. \quad (13)$$

The scalar spectral tilt is [32,35]

$$n_s - 1 = \frac{d \ln P_\zeta}{d \ln k} \approx 3 - |2\eta_H - 3| - \frac{2(2\eta_H^2 - 9\eta_H + 6)\epsilon_H}{|2\eta_H - 3|}. \quad (14)$$

In the same way, we can obtain the power spectrum of the tensor perturbation, and the tensor to scalar ratio is [32,35]

$$r \approx 2^{3-|2\eta_H-3|} \left( \frac{\Gamma[3/2]}{\Gamma[|2\eta_H-3|/2]} \right)^2 16\epsilon_H. \quad (15)$$

If we neglect the contribution of  $\epsilon_H$  in Equations (14) and (15), there exists a duality between  $\eta_H = \alpha$  and  $\eta_H = 3 - \alpha$  as discussed in Refs. [13,14], where  $\alpha$  is a small constant.

### 3. Duality in Tachyon Inflation

In this section, we review the tachyon inflation. The action of the tachyon field is

$$S_T = - \int d^4x \sqrt{-g} V(T) \sqrt{1 + g^{\mu\nu} \partial_\mu T \partial_\nu T}. \quad (16)$$

The background equations are where  $T$  stands for the tachyon field, and  $V(T)$  is the potential. The background equations are

$$H^2 = \frac{1}{3} \frac{V}{\sqrt{1-\dot{T}^2}}, \quad (17)$$

$$\frac{\ddot{T}}{1-\dot{T}^2} + 3H\dot{T} + \frac{V_{,T}}{V} = 0, \quad (18)$$

$$\dot{H} = -\frac{3}{2}H^2\dot{T}^2. \quad (19)$$

Similar to the canonical inflation, for the tachyon inflation, we also define the Hubble flow slow-roll parameters [26,36],

$${}^n\beta_H = \frac{2}{3H^2} \left( \frac{(H_{,T})^{n-1} H^{(n+1)}}{H^n} \right)^{1/n}, \quad (20)$$

where  $H^{(n)} = d^n H / dT^n$ . Compared to the canonical definition (5), extra  $1/H^2$  factor is added for the tachyon field. The first two slow-roll parameters are

$$\epsilon_H = \frac{2}{3H^2} \left( \frac{H_{,T}}{H} \right)^2, \quad (21)$$

$$\eta_H = \frac{2H_{,TT}}{3H^3}. \quad (22)$$

Just like the constant condition (7) in canonical inflation, for the tachyon inflation, we also take the slow-roll parameter  $\eta_H$  as a constant,

$$\eta_H = \text{Constant}. \quad (23)$$

On the other hand, we can define the horizon flow slow-roll parameters [37],

$$\epsilon_0 = \frac{H_0}{H}, \quad \epsilon_{i+1} = -\frac{d \ln |\epsilon_i|}{dN}, \quad (24)$$

where  $N$  is the  $e$ -folding numbers. With the help of the background Equations (17) and (18), we can obtain the relation between the Hubble flow slow-roll parameters and the horizon flow slow-roll parameters,

$$\epsilon_H = \epsilon_1, \quad \eta_H = 2\epsilon_1 - \frac{1}{2}\epsilon_2. \quad (25)$$

From background equations and the slow-roll parameter, we can obtain the number of  $e$ -folds before the end of inflation,

$$N = \int_t^{t_f} H(t) dt = \pm \sqrt{\frac{3}{2}} \int_T^{T_f} \frac{H}{\sqrt{\epsilon_1}} dT, \quad (26)$$

where  $t$  is the cosmic time, and the subscript  $f$  denotes the end of inflation, the  $\pm$  sign is the same as the sign of  $\dot{T}$ .

### 3.1. The Scalar Perturbation

In the flat gauge  $\delta T(x, t) = 0$ , using the canonically normalized field  $v = z\zeta$ , the gravitational action plus the tachyon action for the curvature perturbation  $\delta g_{ij} = a^2(1 + 2\zeta)\delta_{ij}$  becomes

$$S = \int d^3x d\tau \frac{1}{2} \left[ v'^2 - c_s^2 (\partial_i v)^2 + \frac{z''}{z} v^2 \right], \quad (27)$$

where the effective sound speed is  $c_s^2 = 1 - 2\epsilon_1/3$  [27], and

$$z = \frac{\sqrt{3}a\dot{T}}{\sqrt{1 - \dot{T}^2}}. \quad (28)$$

The Mukhanov-Sasaki equation is [29],

$$v_k'' + \left( c_s^2 k^2 - \frac{z''}{z} \right) v_k = 0. \quad (29)$$

To solve it, we need transfer it to the Bessel equation form

$$v_k'' + \left( c_s^2 k^2 - \frac{\nu^2 - 1/4}{\tau^2} \right) v_k = 0. \quad (30)$$

Assuming that  $\nu$  is a constant, the power spectrum of the scalar perturbation for the tachyon inflation can be obtained by the Bessel method, and the result is

$$P_\zeta = \frac{k^3}{2\pi^2} |\zeta_k|^2 = \frac{2^{2\nu-3}}{2c_s\epsilon_1} \left[ \frac{\Gamma(\nu)}{\Gamma(3/2)} \right]^2 \left( 1 + \frac{\epsilon_1}{1 - \epsilon_2} \right)^{1-2\nu} \left( \frac{H}{2\pi} \right)^2 \left( \frac{c_s k}{aH} \right)^{3-2\nu} \Big|_{c_s k = aH}. \quad (31)$$

The scalar tilt is

$$n_s - 1 = \frac{d \ln P_\zeta}{d \ln k} = 3 - 2\nu. \quad (32)$$

For the constant-roll condition (23), to the first order of  $\epsilon_1$ , the value of  $\nu$  in Equation (30) is

$$\nu \approx \frac{1}{2} |3 - \eta_H| + \frac{(16\eta_H^3 - 40\eta_H^2 - 15\eta + 27)\epsilon_1}{3|3 - \eta_H|(2\eta_H + 1)}. \quad (33)$$

Substituting Equation (33) into Equation (32), we obtain [26]

$$n_s \approx 4 - |3 - 2\eta_H| + \frac{(-32\eta_H^3 + 80\eta_H^2 + 30\eta_H - 54)\epsilon_1}{3|3 - 2\eta_H|(2\eta_H + 1)}, \quad (34)$$

### 3.2. The Tensor Perturbation

For the tensor perturbation  $\delta g_{ij} = a^2 \gamma_{ij}$ , to the second order, the gravitational action plus the tachyon action becomes

$$S = \frac{1}{8} \int d^4x \left[ a^3 (\dot{\gamma}_{ij})^2 - a (\gamma_{ij,k})^2 \right], \quad (35)$$

where  $\gamma_{ij} = \sum_{s=+, \times} e_{ij}^s \gamma^s$ . Similar to the scalar perturbation, the power spectrum is

$$P_T = 2^{2\mu} \left[ \frac{\Gamma(\mu)}{\Gamma(3/2)} \right]^2 \left( 1 + \frac{\epsilon_1}{1 - \epsilon_2} \right)^{1-2\mu} \left( \frac{H}{2\pi} \right)^2 \left( \frac{k}{aH} \right)^{3-2\mu}, \quad (36)$$

where

$$\mu^2 = \frac{1}{4} + \frac{a''}{a} \tau^2. \quad (37)$$

Combining Equations (31) and (36), to the first order of  $\epsilon_1$ , we obtain the tensor-to-scalar ratio

$$r = 2^{2(\mu-\nu)+4} \left[ \frac{\Gamma(\mu)}{\Gamma(\nu)} \right]^2 \epsilon_1. \quad (38)$$

For the constant-roll condition (23), to the first order of  $\epsilon_1$ , the value of  $\mu$  in Equation (37) is

$$\mu \approx \frac{3}{2} + \frac{3 - 2\eta_H}{3(1 + 2\eta_H)} \epsilon_1. \quad (39)$$

Substituting it into Equation (38), we obtain the tensor-to-scalar ration with the constant-roll condition [26],

$$r \approx 2^{3-|3-2\eta_H|} \left( \frac{\Gamma[3/2]}{\Gamma[|3-2\eta_H|/2]} \right)^2 16\epsilon_1. \quad (40)$$

### 3.3. The Duality and Observation

The condition of small  $\eta_H$  of the tachyon inflation can be expressed as

$$\eta_H = \alpha, \quad (41)$$

where  $|\alpha| \ll 1$  is small, and this situation is also the slow-roll inflation. Substituting the small  $\eta_H$  condition (41) into the scalar tilt (34) and tensor-to-scalar ratio (40), we get

$$n_s - 1 = 2\alpha - 4\epsilon_1, \quad (42)$$

$$r = 16\epsilon_1. \quad (43)$$

On the other hand, the large  $\eta_H$  condition is

$$\eta_H = 3 - \alpha, \quad (44)$$

and this situation is called ultra-slow-roll inflation. By using this condition, the scalar tilt and tensor-to-scalar ratio becomes

$$n_s - 1 = 2\alpha - \frac{54}{7}\epsilon_1, \quad (45)$$

$$r = 16\epsilon_1. \quad (46)$$

If  $\epsilon_1$  can be neglected, Equation (42) is equal to Equation (45), and Equation (43) is equal to Equation (46). Therefore, the scalar tilt and tensor-to-scalar ratio are the same between the small and large  $\eta_H$ . This denotes that there exists a duality between the slow-roll and the ultra slow-roll tachyon inflation

Combining the constant condition (23) and the relation (25), we can obtain the slow parameter  $\epsilon_1$ ,

$$\epsilon_1(N) = \frac{\eta_H \exp(2\eta_H N)}{2 \exp(2\eta_H N) + C_1}, \quad (47)$$

where  $C_1$  is the integration constant. For the slow-roll condition with  $\eta_H \ll 1$ , the inflation can exit gracefully. In this case, the integration constant can be determined by the condition  $\epsilon_1(N = 0) = 1$ , and the slow parameter (48) becomes

$$\epsilon_1(N) = \frac{\eta_H \exp(2\eta_H N)}{2 \exp(2\eta_H N) + \eta_H - 2}. \quad (48)$$

For the ultra-slow roll condition with  $\epsilon_H \approx 3$ , the slow-roll parameter  $\epsilon_1$  decreases along with the time, the inflation cannot exit, and the integration constant  $C_1$  cannot be determined in this situation. Because the inflation cannot exit, the  $e$ -folds  $N_{\text{ultra}}$  before the end of inflation cannot be defined well. In this situation, the  $e$ -folds  $N_{\text{ultra}}$  and the integration constant  $C_1$  are defined to make the slow-roll parameter  $\epsilon_1$  the same as Equation (48) where the difference is that  $\eta_H$  is replaced by  $3 - \eta_H$  in consideration of the ultra-slow-roll condition.

Substituting Equation (48) into scalar tilt (34) and tensor-to-scalar ratio (40), and comparing them with the Planck 2018 [2,8] observational data, we can obtain the constraints on the slow-roll parameter  $\eta_H$ , and the results are displayed in Figures 1 and 2. Figure 1 shows the parametric space corresponding to a small  $\eta_H$  case. In the left panel, we show the contours for  $n_s$  and  $r$ . The inner contour shows the bounds of Planck 2018 68% confidence level, whereas the outer contour represents the region with a 95% confidence level. The red

and green on the color maps are the regions that correspond to observational constraints on the constant-roll inflationary models. In the right panel, we present the plot between  $\eta_H$  and  $N$  where  $N$  represents the number of  $e$ -folding. Figure 2 shows the results for the large  $\eta$  case. The color coding here is the same as in Figure 1. From the figures, we can see the duality between the constant-roll tachyon inflation with large and small  $\eta_H$  exit.

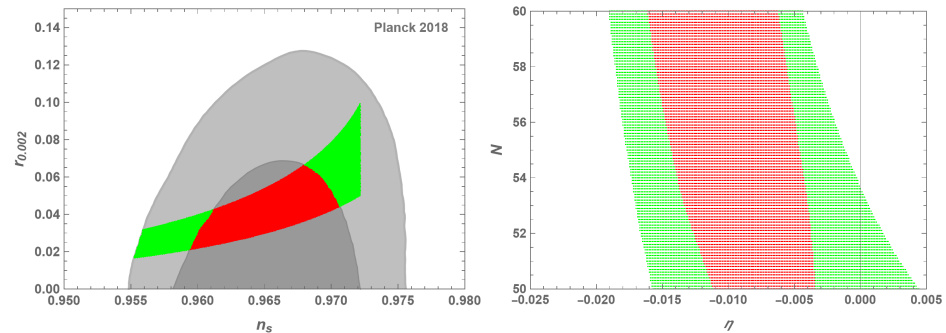


**Figure 1.** (Left panel) shows the marginalized 68%, and 95% confidence level contours for  $n_s$  and  $r$  from Planck 2018 and the observational constraints on the constant-roll inflationary models whereas the (Right panel) shows observational constraints on  $\eta_H$  and  $N$  for 68% (red) and 95% (green) C.L.s, respectively for small  $\eta_H$ .

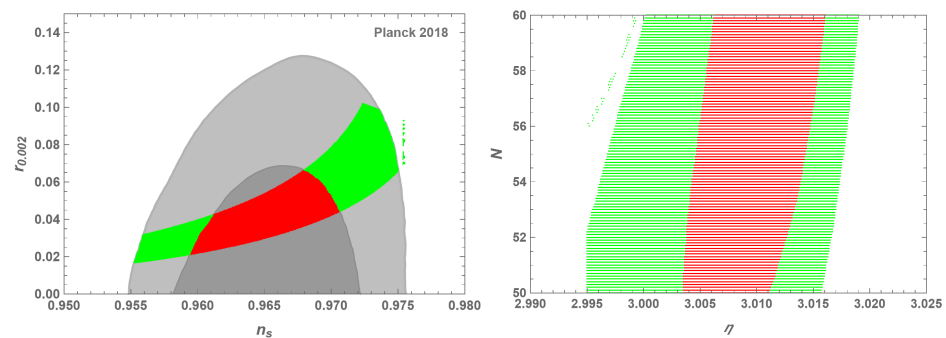


**Figure 2.** (Left panel) shows the marginalized 68%, and 95% confidence level contours for  $n_s$  and  $r$  from Planck 2018 and the observational constraints on the constant-roll inflationary models whereas the (Right panel) shows observational constraints on  $\eta_H$  and  $N$  for 68% (red) and 95% (green) C.L.s, respectively for large  $\eta_H$ .

In Figure 3, we compare the difference of  $n_s$  and  $r$  between the tachyon inflation models with large  $\eta$  and small  $\eta$ , where the  $e$ -folds are  $N = 60$ . The black line corresponds to the result of the tachyon inflation with small  $\eta_H$ , and the green dots are the results from the tachyon inflation with large  $\eta_H$ . The tachyon inflation models with large and small  $\eta_H$  giving almost the same scalar tilt  $n_s$  and tensor-to-scalar ratio  $r$ . In Figure 3, to give the same pair of  $n_s$  and  $r$ , the small  $\eta_s$  and the large  $\eta_l$  almost satisfy  $\eta_s + \eta_l \approx 3$  for the whole black line, which is the robust evidence of the duality between the large and small  $\eta$ .

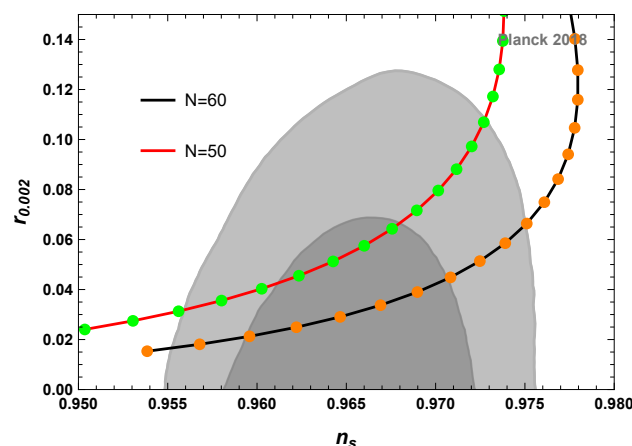


**Figure 3.** The difference of  $n_s$  and  $r$  between the tachyon inflation models with large  $\eta$  and small  $\eta$ . The black line is the results from the tachyon inflation with small  $\eta$ , and the green dots are the results from the large  $\eta$ .

#### 4. Conclusions

To conclude, we have investigated the constant-roll tachyon inflation with large and small  $\eta$ . We neglect the contribution of the first slow-roll parameter  $\epsilon_H$ , which is a reasonable assumption for the constant roll inflationary models with  $\epsilon_H$  decreasing during inflation. In that case, a duality exists for the expressions of  $n_s$  and  $r$  for small and large  $\eta$ . We also use observational data to constrain the constant-roll inflationary models. By fitting the spectral index  $n_s$  and tensor to scalar ratio  $r$ , with the observations, we get small and large  $\eta$  in this range  $-0.01629 \leq \eta \leq -0.00079$  and  $3.00081 \leq \eta \leq 3.01621$  at the  $2\sigma$  C.L for  $N = 60$  e-folding.

**Author Contributions:** All authors are contributed equally. All authors have read and agreed to the published version of the manuscript.

**Funding:** This research was supported in part by the National Natural Science Foundation of China under Grant No. 11947138, Talent introduction fund of Hubei Polytechnic University under Grant No. 20xjz02R.

**Institutional Review Board Statement:** Not applicable.

**Informed Consent Statement:** Not applicable.

**Data Availability Statement:** Not applicable.

**Conflicts of Interest:** The authors declare no conflict of interest.

#### References

1. Spergel, D.N.; Spergel, D.N.; Bean, R.; Doré, O.; Nolta, M.R.; Bennett, C.L.; Dunkley, J.; Hinshaw, G.; Jarosik, N.; Komatsu, E.; et al. Three-Year Wilkinson Microwave Anisotropy Probe (WMAP) Observations: Implications for Cosmology. *Astrophys. J. Suppl.* **2007**, *170*, 377. [[CrossRef](#)]
2. Akrami, Y.; Arroja, F.; Ashdown, M.; Aumont, J.; Baccigalupi, C.; Ballardini, M.; Banday, A.J.; Barreiro, R.B.; Bartolo, N.; Basak, S.; et al. Planck 2018 results. X. Constraints on inflation. *Astron. Astrophys.* **2020**, *641*, A10.
3. Guth, A.H. The Inflationary Universe: A Possible Solution to the Horizon and Flatness Problems. *Phys. Rev. D* **1981**, *23*, 347. [[CrossRef](#)]
4. Linde, A.D. A New Inflationary Universe Scenario: A Possible Solution of the Horizon, Flatness, Homogeneity, Isotropy and Primordial Monopole Problems. *Phys. Lett. B* **1982**, *108*, 389–393. [[CrossRef](#)]
5. Albrecht, A.; Steinhardt, P.J. Cosmology for Grand Unified Theories with Radiatively Induced Symmetry Breaking. *Phys. Rev. Lett.* **1982**, *48*, 1220. [[CrossRef](#)]
6. Starobinsky, A.A. A New Type of Isotropic Cosmological Models Without Singularity. *Phys. Lett.* **1980**, *91*, 99–102. [[CrossRef](#)]
7. Guth, A.H.; Pi, S.Y. Fluctuations in the New Inflationary Universe. *Phys. Rev. Lett.* **1982**, *49*, 1110. [[CrossRef](#)]
8. Array, K.; BICEP2 Collaborations; Ade, P.A.R.; Ahmed, Z.; Aikin, R.W.; Alexander, K.D.; Barkats, D.; Benton, S.J.; Bischoff, C.A.; Bock, J.J.; et al. (BICEP2, Keck Array). BICEP2 / Keck Array X: Constraints on Primordial Gravitational Waves using Planck, WMAP, and New BICEP2/Keck Observations through the 2015 Season. *Phys. Rev. Lett.* **2018**, *121*, 221301.

9. Martin, J.; Motohashi, H.; Suyama, T. Ultra Slow-Roll Inflation and the non-Gaussianity Consistency Relation. *Phys. Rev. D* **2013**, *87*, 023514. [[CrossRef](#)]
10. Motohashi, H.; Starobinsky, A.A.; Yokoyama, J. Inflation with a constant rate of roll. *J. Cosmol. Astropart. Phys.* **2015**, *1509*, 018. [[CrossRef](#)]
11. Tsamis, N.C.; Woodard, R.P. Improved estimates of cosmological perturbations. *Phys. Rev. D* **2004**, *69*, 084005. [[CrossRef](#)]
12. Kinney, W.H. Horizon crossing and inflation with large  $\eta$ . *Phys. Rev. D* **2005**, *72*, 023515. [[CrossRef](#)]
13. Tzirakis, K.; Kinney, W.H. Inflation over the hill. *Phys. Rev. D* **2007**, *75*, 123510. [[CrossRef](#)]
14. Morse, M.J.P.; Kinney, W.H. Large- $\eta$  Constant-Roll Inflation Is Never An Attractor. *Phys. Rev. D* **2018**, *97*, 123519. [[CrossRef](#)]
15. Motohashi, H.; Starobinsky, A.A. Constant-roll inflation: confrontation with recent observational data. *EPL* **2017**, *117*, 39001. [[CrossRef](#)]
16. Gao, Q. The observational constraint on constant-roll inflation. *Sci. China Phys. Mech. Astron.* **2018**, *61*, 070411. [[CrossRef](#)]
17. Ghersi, J.T.G.; Zucca, A.; Frolov, A.V. Observational Constraints on Constant Roll Inflation. *J. Cosmol. Astropart. Phys.* **2019**, *5*, 030. [[CrossRef](#)]
18. Gerbino, M.; Freese, K.; Vagnozzi, S.; Lattanzi, M.; Mena, O.; Giusarma, E.; Ho, S. Impact of neutrino properties on the estimation of inflationary parameters from current and future observations. *Phys. Rev. D* **2017**, *95*, 043512. [[CrossRef](#)]
19. Gomes, C.; Bertolami, O.; Rosa, J.A.G. Inflation with Planck data: A survey of some exotic inflationary models. *Phys. Rev. D* **2018**, *97*, 104061. [[CrossRef](#)]
20. Sen, A.; Rolling tachyon. *J. High Energy Phys.* **2002**, *4*, 048. [[CrossRef](#)]
21. Sen, A.; Tachyon matter. *J. High Energy Phys.* **2002**, *7*, 065. [[CrossRef](#)]
22. Gibbons, G.W. Cosmological evolution of the rolling tachyon. *Phys. Lett. B* **2002**, *537*, 1. [[CrossRef](#)]
23. Padmanabhan, T. Accelerated expansion of the universe driven by tachyonic matter. *Phys. Rev. D* **2002**, *66*, 021301. [[CrossRef](#)]
24. Frolov, A.V.; Kofman, L.; Starobinsky, A.A. Accelerated expansion of the universe driven by tachyonic matter. *Phys. Lett. B* **2002**, *545*, 8. [[CrossRef](#)]
25. Fei, Q.; Gong, Y.; Lin, J.; Yi, Z. The reconstruction of tachyon inflationary potentials. *J. Cosmol. Astropart. Phys.* **2017**, *1708*, 018. [[CrossRef](#)]
26. Gao, Q.; Gong, Y.; Fei, Q. Constant-roll tachyon inflation and observational constraints. *J. Cosmol. Astropart. Phys.* **2018**, *1805*, 005. [[CrossRef](#)]
27. Garriga, J.; Mukhanov, V.F. Perturbations in k-inflation. *Phys. Lett. B* **1999**, *458*, 219–225. [[CrossRef](#)]
28. Hwang, J.-C.; Noh, H. Cosmological perturbations in a generalized gravity including tachyonic condensation. *Phys. Rev. D* **2002**, *66*, 084009. [[CrossRef](#)]
29. Steer, D.A.; Vernizzi, F. Tachyon inflation: Tests and comparison with single scalar field inflation. *Phys. Rev. D* **2004**, *70*, 043527. [[CrossRef](#)]
30. Barbosa-Cendejas, N.; De-Santiago, J.; German, G.; Hidalgo, J.C.; Mora-Luna, R.R. Theoretical and observational constraints on Tachyon Inflation. *J. Cosmol. Astropart. Phys.* **2018**, *3*, 015. [[CrossRef](#)]
31. Liddle, A.R.; Parsons, P.; Barrow, J.D. Formalizing the slow roll approximation in inflation. *Phys. Rev. D* **1994**, *50*, 7222. [[CrossRef](#)] [[PubMed](#)]
32. Yi, Z.; Gong, Y. On the constant-roll inflation. *J. Cosmol. Astropart. Phys.* **2018**, *1803*, 052. [[CrossRef](#)]
33. Mukhanov, V.F. Gravitational Instability of the Universe Filled with a Scalar Field. *JETP Lett.* **1985**, *41*, 493–496.
34. Sasaki, M. Large Scale Quantum Fluctuations in the Inflationary Universe. *Prog. Theor. Phys.* **1986**, *76*, 1036–1046. [[CrossRef](#)]
35. Gao, Q.; Gong, Y.; Yi, Z. On the constant-roll inflation with large and small  $\eta_H$ . *Universe* **2019**, *5*, 215. [[CrossRef](#)]
36. Liddle, A.R.; Turner, M.S. Second order reconstruction of the inflationary potential. *Phys. Rev. D* **1994**, *50*, 758; Erratum in *Phys. Rev. D* **1996**, *54*, 2980. [[CrossRef](#)]
37. Schwarz, D.J.; Terrero-Escalante, C.A.; Garcia, A.A. Higher order corrections to primordial spectra from cosmological inflation. *Phys. Lett. B* **2001**, *517*, 243–249. [[CrossRef](#)]